The trace element conundrum of natural quasicrystals

Simone Tommasini [a], Luca Bindi [a,b], Maurizio Petrelli [c], Paul D. Asimow [d], and Paul J. Steinhardt [e]

SUPPORTING INFORMATION

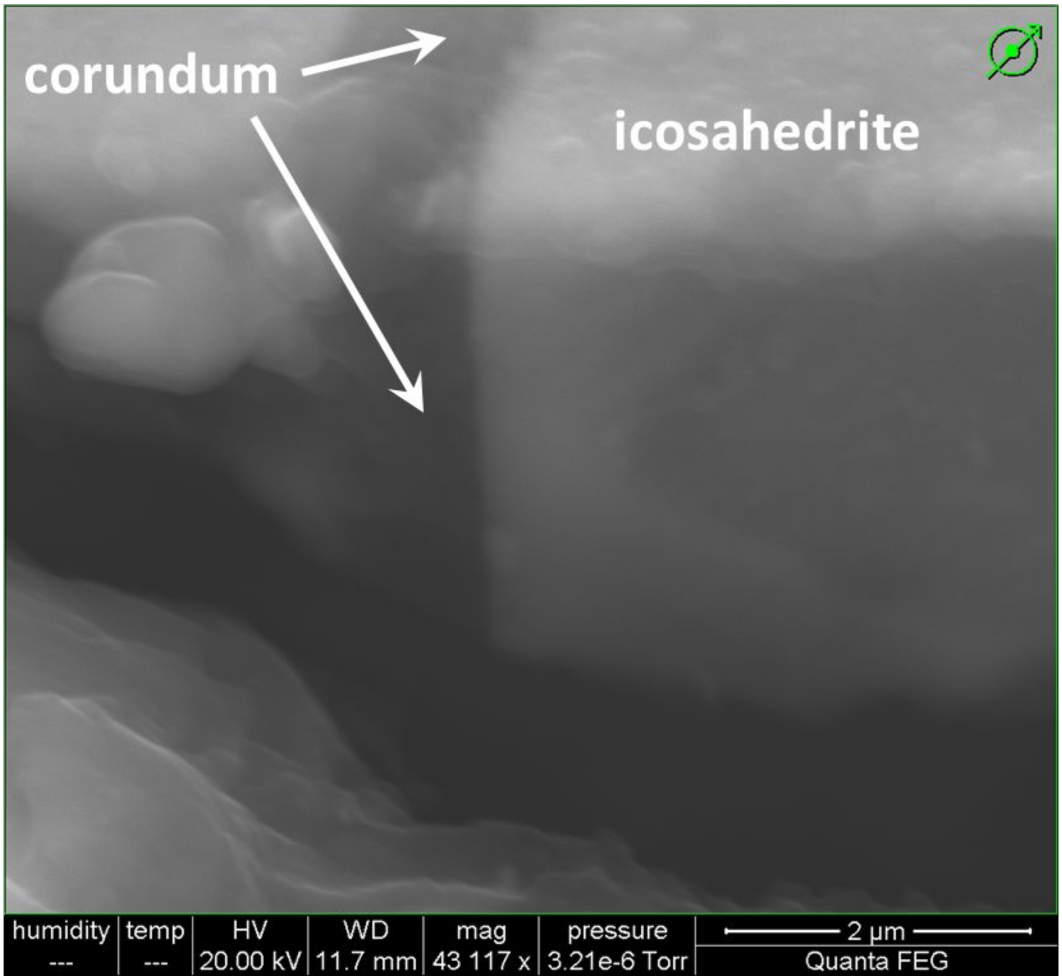

Figure S1 – Nanometric “finger” of corundum penetrating icosahedrite. Scale bar of 2μm is shown at the bottom right.

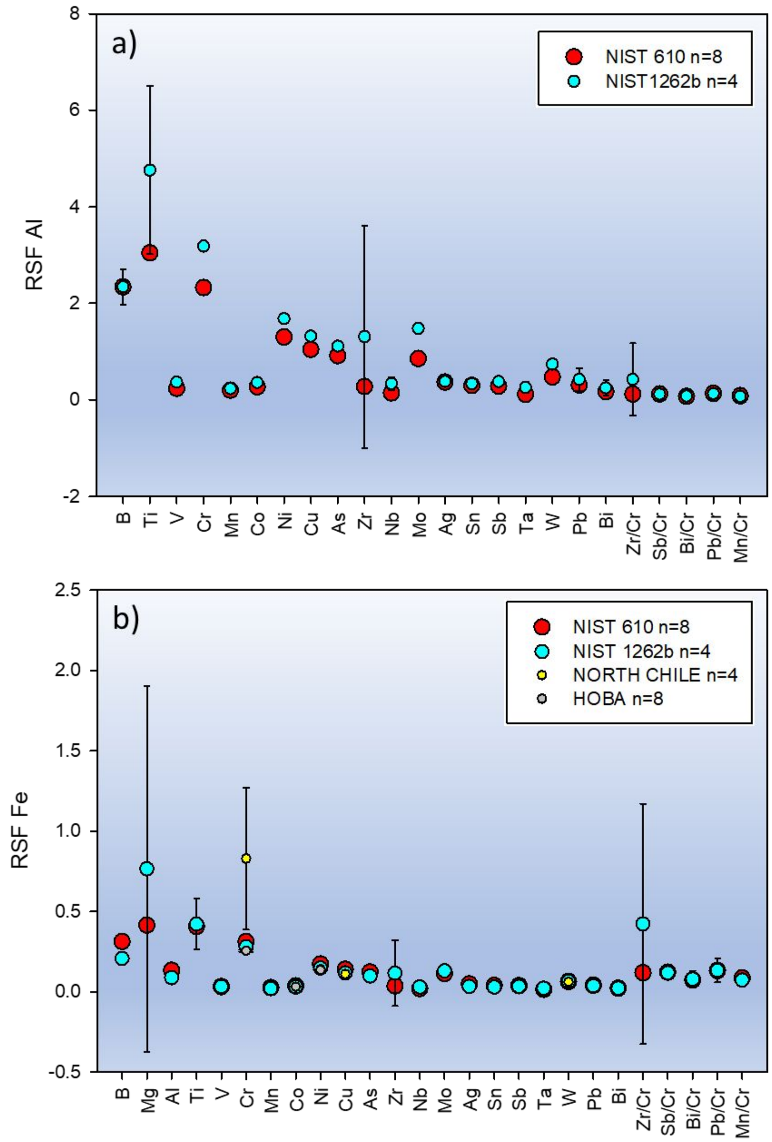

Figure S2 – Relative Sensitivity Factors (RSF) normalized to Al (a) and Fe (b) for NIST SRM 610 silicate glass standard [21] as calibrator reference material, and HOBA, NORTH CHILE and NIST SRM 1262b as metal alloy reference materials. RSF = $(C_i/C_{re})/(Int_i/Int_{re})$, where C_i is the concentration of element *i*, and Int_i is the background-corrected intensity for the peak used for that element; C_{re} is the concentration of the reference element (Al or Fe), and Int_{re} the background-corrected intensity of either Al or Fe. The RSF are reported for those trace elements available in the metal alloy reference materials and are compared to those of the NIST SRM 610 reference material. Both Al-and Fe-normalized RSF of elements and elemental ratios, used in this study, of the metal matrices and silicate glass matrix are in good agreement except for those elements heterogeneously distributed in the metal alloys (e.g., Zr, Ti).

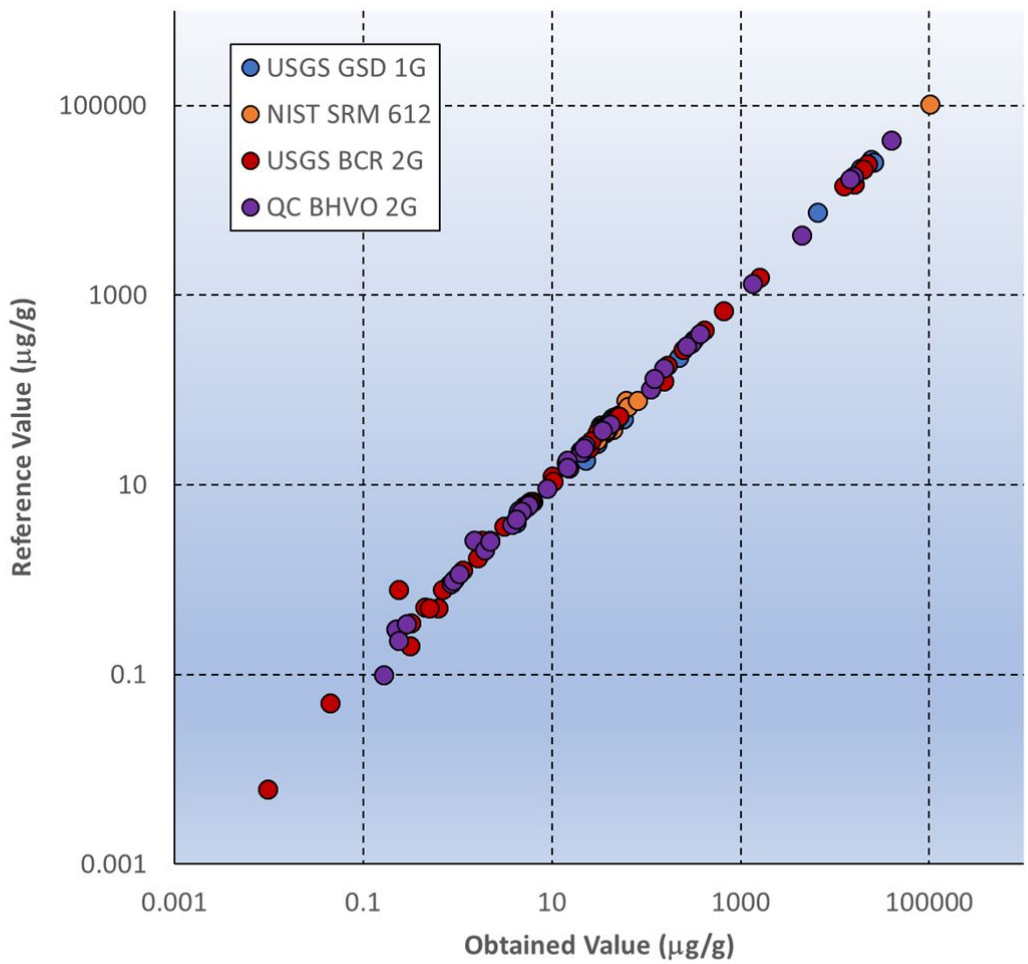

Figure S3 - Quality control diagram showing the elemental contents determined in four reference materials (NIST SRM 612, USGS BCR2G, USGS BHVO2G, and USGS GSD1), [30] and compared to the certified values (see also Table S1).

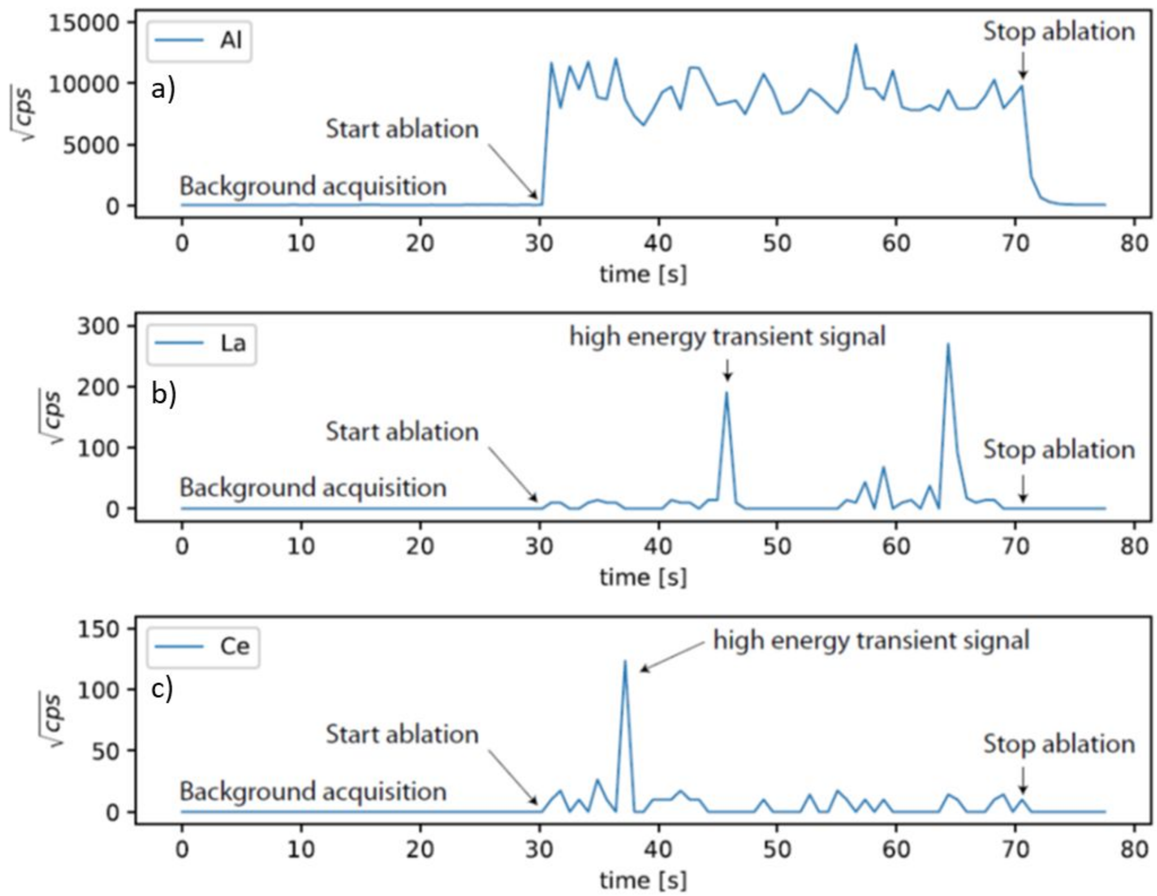

Figure S4 - Time-resolved signals for Al (a), La (b), and Ce (c) of sample NI2_02 (Table 2) acquired during ablation and showing the high-energy transients likely due to the occurrence of nanoparticles in the ablated volume of QCs.

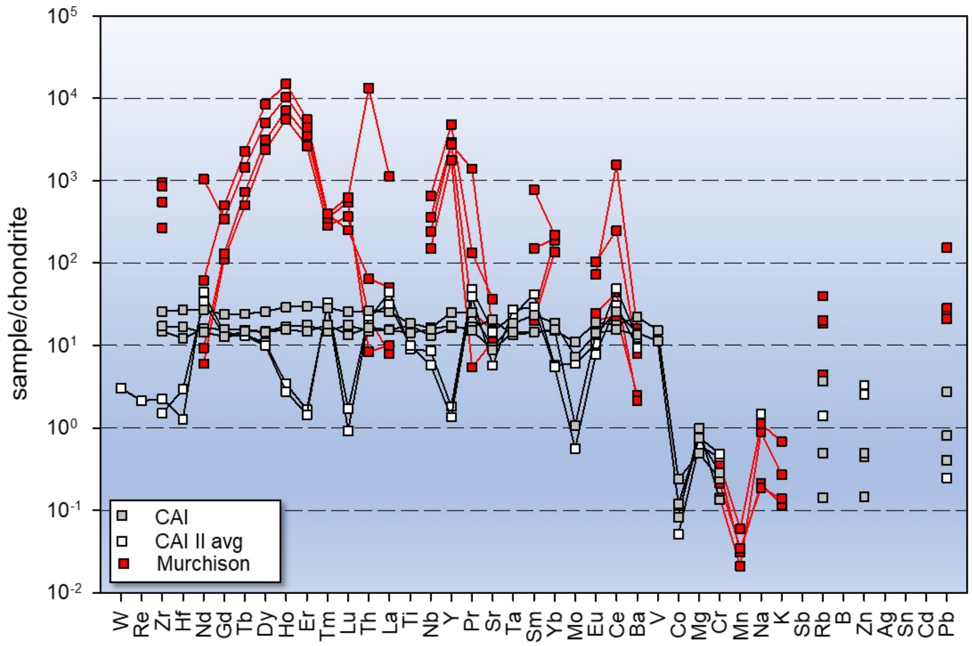

Figure S5– Chondrite normalized [33] trace element spider-diagram of the unique ultra-refractory inclusions in Murchison meteorite [37] and in Group II CAIs [31,35] in comparison with others average CAI composition. [35] The elements are ordered from left to right with decreasing 50% condensation temperature temperature (T_C) in a gas of solar composition at 10^{-4} bar. [32] The complementary fractionation of highly refractory elements is noteworthy and suggests materials processed in a high-temperature nebular environment.

Table S1 – Trace element analyses (μg/g) of reference standards.

Element	Isotope mass	NIST SRM 612	1sd	ref. values	Accuracy %	USGS GSD 1G	1sd	ref. values	Accuracy %	BCR 2G	1sd	ref. values	Accuracy %	BHVO 2G	1sd	ref. values	Accuracy %
B	11	35.0	0.3	35	0%	58	1	50	16%	5.2	0.5	5.8	10%	5	2		
Na	23	101625	850	103858	2%	23950	71	26707	10%	22050	212	23962	8%	15565	233	17806	13%
Mg	25	60	1	77	21%	18660	283	21712	14%	19750	212	21467	8%	39200	990	42994	9%
K	39	64	1	66	3%	25600	990	25300	1%	15950	495	14900	7%	4460	42	4270	4%
Ti	47	42.3	0.5	44	4%	6480	141	7434	13%	12450	212	14100	12%	14385	262	16726	14%
V	51	37.3	0.2	39	4%	38.0	0.3	44	14%	410	10	425	4%	301	9	308	2%
Cr	53	35	1	36	3%	37.1	0.5	42	12%	14	1	17	17%	267	8	293	9%
Mn	55	44.0	0.4	38	16%	222	1	220	1%	1590	14	1550	3%	1349	34	1317	2%
Co	59	34.0	0.3	35	3%	35	1	40	13%	35	1	38	9%	41.2	0.2	44	6%
Zn	66	38.7	0.3	38	2%	50	3	54	7%	153	6	125	22%	112	2	102	10%
Ga	71	36.4	0.2	36	1%	50	1	54	7%	21.5	0.4	23	7%	21	1	22	7%
As	75	33.0	0.5	37	11%	30	1	27	12%	1.0	0.1			0.9	0.2		
Rb	85	31.7	0.3	31	1%	35.2	0.2	37.3	6%	47	1	47	1%	8.9	0.3	9.2	4%
Sr	88	80	1	78	2%	65	2	69.4	6%	320	4	342	6%	370	1	396	7%
Y	89	36.6	0.4	38	4%	37.0	0.4	42	12%	30.3	0.4	35	13%	22.5	0.1	26	13%
Zr	90	37	1	38	3%	38	1	42	10%	168	3	184	9%	153.3	0.2	170	10%
Nb	93	34.5	0.1	40	14%	35.0	0.4	42	17%	10.0	0.2	13	20%	14.5	0.6	18	21%
Mo	95	35.9	0.3	38	6%	33	1	39	15%	248	9	270	8%	3.7	0.4	3.8	2%
Ag	107	21.1	0.4	22	4%	20.2	0.3	23	12%	0.627		0.5	25%	0.84	0.02		
Cd	111	28.1	0.4	28	1%	23	2	18	26%	0.31	0.00	0.2	55%	0.16	0.07	0.1	64%
Sn	120	35	1	38	9%	29	1	29	0%	1.83	0.04	2.6	30%	1.5	0.0	2.6	42%
Sb	121	31.4	0.2	38	17%	33	1	43	24%	0.32	0.01	0.4	8%	0.22	0.01	0.3	27%
Ba	137	38.3	0.2	40	4%	63.0	0.1	67	6%	665	35	683	3%	121	6	131	7%
La	139	37.5	0.2	36	5%	36.5	0.7	39	6%	25	1	25	1%	14.6	0.4	15	4%
Ce	140	37	1	39	3%	37.1	0.6	41.4	10%	51	2	53	4%	34	1	38	9%
Pr	141	35.8	0.5	37	4%	38.6	0.2	45	14%	6.1	0.4	6.7	9%	4.5	0.1	5.4	16%
Nd	145	34.9	0.4	36	3%	39.8	0.0	44.7	11%	26	2	29	11%	22	1	25	11%
Sm	147	36	1	38	4%	41.7	0.0	47.8	13%	5.8	0.3	6.6	13%	5.58	0.01	6.1	9%
Eu	153	36	1	35	4%	38.0	0.6	41	7%	1.83	0.08	2.0	7%	1.96	0.02	2.1	6%
Gd	157	36	1	37	1%	43.7	0.4	50.7	14%	5.8	0.3	6.7	13%	5.6	0.3	6.2	9%
Tb	159	37	1	36	2%	43.1	0.2	47	8%	0.93	0.09	1.0	9%	0.85	0.03	0.9	7%
Dy	163	33.9	0.5	36	6%	44.8	0.1	51.2	13%	5.6	0.1	6	12%	4.8	0.3	5.3	10%
Ho	165	37.0	0.4	38	3%	44.1	0.1	49	10%	1.14	0.02	1.3	11%	0.90	0.01	1.0	8%
Er	166	34.6	0.4	38	9%	32.4	0.1	40.1	19%	3.1	0.1	3.7	16%	2.18	0.04	2.6	15%
Tm	169	34	1	38	11%	42.0	0.3	49	14%	0.45	0.04	0.5	12%	0.29	0.01	0.3	16%
Hf	178	35	1	35	0%	35.8	0.4	39	8%	4.4	0.4	4.8	10%	4.19	0.06	4.3	3%
Ta	181	37	1	40	8%	38.1	0.5	40	5%	0.69	0.03	0.8	11%	1.04	0.01	1.2	9%
W	182	38.0	0.5	40	5%	38.2	0.1	43	11%	0.500	0.001	0.5	0%	0.24	0.02	0.2	3%
Re	185	6.3	0.1	6.6	5%	4.3	0.1			0.0098		0.01		bdl		0.0005	
Tl	205	15.0	0.1	15	1%	0.81	0.05	0.9	10%	0.24	0.02	0.3	22%	0.027	0.006		
Pb	208	38	1	39	3%	46	2	50	9%	10.4	0.4	11	5%	1.72	0.02	1.7	1%
Bi	209	30	1	30	1%	30	1	35	13%	0.05		0.05	10%	0.04		0.01	310%
Th	232	36	1	38	4%	39	2	41	5%	5.4	0.3	5.9	8%	1.11	0.03	1.2	9%

Table S2 - First Stage: end member *proxies* and trace element content (CI normalized) of the mixing process

end member *proxies*			Zr	Nd	Er	Tm	Cr	Zr/Cr	Tm/Er	Nd/Er
Murchison avg 1-3			902	7.67	3069	319	0.26	3477	0.104	0.0025
CI			1	1	1	1	1			
avg CAI II			1.88	39.01	1.55	32.30	0.46	4.09	20.77	25.09
avg CAI			19.31	19.14	20.72	20.42	0.22	88.2	0.99	0.92
CAI II 20%-CI 80%			1.18	8.60	1.11	7.26	0.89	1.32	6.53	7.74
mixtures						**barren decagonite**				
CAI II	**CI**									
100%	0%		1.88	39.01	1.55	32.30	0.46	4.09	20.77	25.09
80%	20%		1.70	31.41	1.44	26.04	0.57	3.00	18.03	21.75
60%	40%		1.53	23.81	1.33	19.78	0.68	2.26	14.84	17.86
40%	60%		1.35	16.21	1.22	13.52	0.78	1.72	11.06	13.26
20%	**80%**		**1.18**	**8.60**	**1.11**	**7.26**	**0.89**	**1.32**	**6.53**	**7.74**
0%	100%		1	1	1	1	1	1	1	1
CAI II-CI	**Murchison**	**% nanoparticles**								
100%	0%	3%	0.035	0.258	0.033	0.218	0.0268	1.32	6.53	7.74
99.95%	0.05%	3%	0.049	0.258	0.079	0.222	0.0268	1.82	2.80	3.25
99.8%	0.2%	3%	0.089	0.258	0.217	0.236	0.0267	3.34	1.09	1.19
99.5%	0.5%	3%	0.170	0.258	0.494	0.264	0.0267	6.39	0.54	0.52
99%	1%	3%	0.305	0.258	0.954	0.311	0.0266	11.5	0.33	0.27
98%	**2%**	**3%**	**0.575**	**0.258**	**1.874**	**0.405**	**0.0264**	**21.8**	**0.22**	**0.14**
95%	**5%**	**3%**	**1.386**	**0.257**	**4.636**	**0.685**	**0.0258**	**53.7**	**0.15**	**0.06**
90%	10%	3%	2.736	0.255	9.238	1.152	0.0249	110	0.12	0.028
80%	20%	3%	5.437	0.253	18.44	2.085	0.0230	237	0.11	0.014
0%	100%	3%	27.05	0.230	92.08	9.555	0.0078	3477	0.10	0.002
CAI II	**Murchison**	**% nanoparticles**								
100%	0%	3%	0.056	1.170	0.047	0.969	0.0138	4.09	20.8	25.1
99.9%	0.1%	3%	0.083	1.169	0.139	0.978	0.0138	6.05	7.05	8.43
99.8%	0.2%	3%	0.110	1.169	0.231	0.986	0.0138	8.01	4.27	5.06
99.5%	0.5%	3%	0.191	1.166	0.507	1.012	0.0138	13.9	2.00	2.30
99%	1%	3%	0.326	1.161	0.967	1.055	0.0137	23.7	1.09	1.20
98%	**2%**	**3%**	**0.596**	**1.152**	**1.887**	**1.141**	**0.0137**	**43.6**	**0.60**	**0.61**
97%	**3%**	**3%**	**0.866**	**1.142**	**2.808**	**1.227**	**0.0136**	**63.6**	**0.44**	**0.41**
95%	**5%**	**3%**	**1.406**	**1.123**	**4.649**	**1.398**	**0.0135**	**104**	**0.30**	**0.24**
93%	**7%**	**3%**	**1.946**	**1.105**	**6.489**	**1.570**	**0.0134**	**145**	**0.24**	**0.17**
90%	10%	3%	2.755	1.076	9.250	1.828	0.0132	209	0.20	0.12
80%	20%	3%	5.454	0.982	18.45	2.686	0.0126	433	0.15	0.053
70%	30%	3%	8.153	0.888	27.66	3.545	0.0120	680	0.13	0.032
0%	100%	3%	27.05	0.230	92.08	9.555	0.0078	3477	0.10	0.002
						barren icosahedrite				
CAI II	**CAI**	**% nanoparticles**								
100%	0%	3%	0.056	1.170	0.047	0.969	0.0138	4.09	20.8	25.1
90%	10%	3%	0.109	1.111	0.104	0.933	0.0131	8.31	8.96	10.7
80%	20%	3%	0.161	1.051	0.162	0.898	0.0124	13.0	5.55	6.50
70%	30%	3%	0.213	0.992	0.219	0.862	0.0116	18.3	3.93	4.53
60%	40%	3%	0.266	0.932	0.277	0.826	0.0109	24.4	2.99	3.37
50%	**50%**	**3%**	**0.318**	**0.872**	**0.334**	**0.791**	**0.0102**	**31.2**	**2.37**	**2.61**
40%	**60%**	**3%**	**0.370**	**0.813**	**0.392**	**0.755**	**0.0095**	**39.1**	**1.93**	**2.08**
30%	**70%**	**3%**	**0.422**	**0.753**	**0.449**	**0.719**	**0.0087**	**48.4**	**1.60**	**1.68**
20%	**80%**	**3%**	**0.475**	**0.693**	**0.506**	**0.684**	**0.0080**	**59.2**	**1.35**	**1.37**
10%	90%	3%	0.527	0.634	0.564	0.648	0.0073	72.3	1.15	1.12
0%	100%	3%	0.579	0.574	0.621	0.612	0.0066	88.2	0.99	0.92

footnote: bold digits are the composites indicated in Figures 5 and 6.

Table S3 - Second Stage: starting material, partition coefficients (Ds), and trace element content (CI normalized) at different aggregated vapor mass fractions (F)

Starting material		**Cr**	**Sb**	**Pb**	**Bi**	**Sb/Cr**	**Bi/Cr**	**Pb/Cr**
CI		1	1	1	1			
avg SCS		1.61	4.40	13.66	8.63	2.73	5.35	8.47
SCS P117		1.83	8.59	73.1	62.5	4.71	34.2	40.0
SCS P56		1.30	13.91	8.26	3.86	10.66	2.96	6.34
Partition coefficient (D) estimates at different F								
F=5%		1	0.00836	0.02326	0.01061			
F=1%		1	0.00165	0.00465	0.00210			
F=0.1%		1	0.00016	0.00046	0.00021			
Aggregated fractional evaporation - CI collision								
	% nanoparticles							
F=5%	1%	0.010	0.200	0.178	0.198	19.96	19.84	17.79
F=1%	1%	0.010	0.998	0.885	0.992	99.8	99.2	88.5
F=0.1%	1%	0.010	9.98	8.84	9.92	998	992	884
Aggregated fractional evaporation - avg SCS collision								
	% nanoparticles							
F=5%	1%	0.016	0.878	2.431	1.712	54.5	106	151
F=1%	0.3%	0.005	1.317	3.627	2.567	272	531	750
F=0.1%	0.5%	0.008	21.96	60.38	42.78	2723	5305	7489
Aggregated fractional evaporation - SCS sample AAS-38-207-P117 collision								
	% nanoparticles							
F=5%	1%	0.018	1.715	13.01	12.394	93.9	679	713
F=1%	0.3%	0.005	2.143	16.18	15.49	469	3393	3544
F=0.1%	0.1%	0.002	8.57	64.63	61.95	4694	33926	35398
Aggregated fractional evaporation - SCS sample AAS-62-61-P56 collision								
	% nanoparticles							
F=5%	1%	0.013	2.775	1.471	0.766	213	58.7	113
F=1%	1%	0.013	13.87	7.31	3.83	1064	294	561
F=0.1%	0.2%	0.003	27.75	14.61	7.66	10638	2936	5602

Supplementary Text

A note on synthetic *vs* natural QCs – Reflected light images of the two specimens of synthetic icosahedrite and two specimens of synthetic decagonite are shown in Figure S6. All the syntheses were via solid state reaction beginning from high-purity metals, namely: (i) icosahedral $Al_{63}Cu_{24}Fe_{13}$ (atomic %) synthesized in Ar at 980 °C and annealed for several hours at 850 °C (labeled SI1; SI = synthetic icosahedrite); (ii) icosahedral $Al_{65}Cu_{23}Fe_{12}$ (atomic %) from the Sigma-Aldrich Company (#757934-10G), synthesized in Ar at 800 °C (labeled SI2); (iii) decagonal $Al_{72}Ni_{24}Fe_4$ (atomic %) from the Goodfellow Company (particle diameter <500 μm), synthesized in Ar at 1350 °C (labeled SD1; SD = synthetic decagonite); (iv) decagonal $Al_{72}Ni_{24}Fe_4$ (atomic %) synthesized in Ar at 1400 °C for 10 hours, quenched, reground, fired again at 1400 °C for 6 hours, and finally quenched (labeled SD2).

The major and trace element analyses of the four synthetic quasicrystals are reported in Tables S4 and S5, respectively. The trace element content of the Khatyrka QCs is significantly different from that of synthetic QCs; most elements occurring in the Khatyrka QCs are below detection limit in synthetic QCs, and the ratios of natural to synthetic abundance of those few elements occurring in both types of QC deviate significantly from unity (Fig. S7). Synthetic icosahedrite spot analyses contain detectable amounts of Zn, Ag, Sn, Pb and Bi, as expected of a material synthesized from Cu starting material. The source of high levels of boron is unclear; although this element is a common surface contaminant, all the samples have been carefully polished before analysis and the B signal does not decay with continued ablation. The synthetic decagonite spot analyses contain measurable levels of Co, expected for material synthesized from Fe and Ni starting material.

In addition to the trace element analyses and the arguments presented in the Introduction section on the natural origin of the studied QCs, [1,5-8,15] we wish to highlight the following indisputable facts: (i) the first natural quasicrystals samples were unearthed in 1979, whereas quasicrystals were not discovered until 1984, so the occurrence of quasicrystals in the 1979 samples could not have been intentional; (ii) no natural terrestrial source of icosahedrite or decagonite has ever been reported; (iii) as for synthetic samples made on Earth, there is no industrial production of Al-Cu alloys with composition corresponding to icosahedrite, khatyrkite, stolperite, and cupalite because they are too brittle to have practical value; (iv) in fact, the only known materials on Earth with the compositions of the quasicrystalline phases in Khatyrka are those synthetic samples fabricated by chemical/metallurgical companies for specific purposes such as this study, production of which evidently began after 1984.

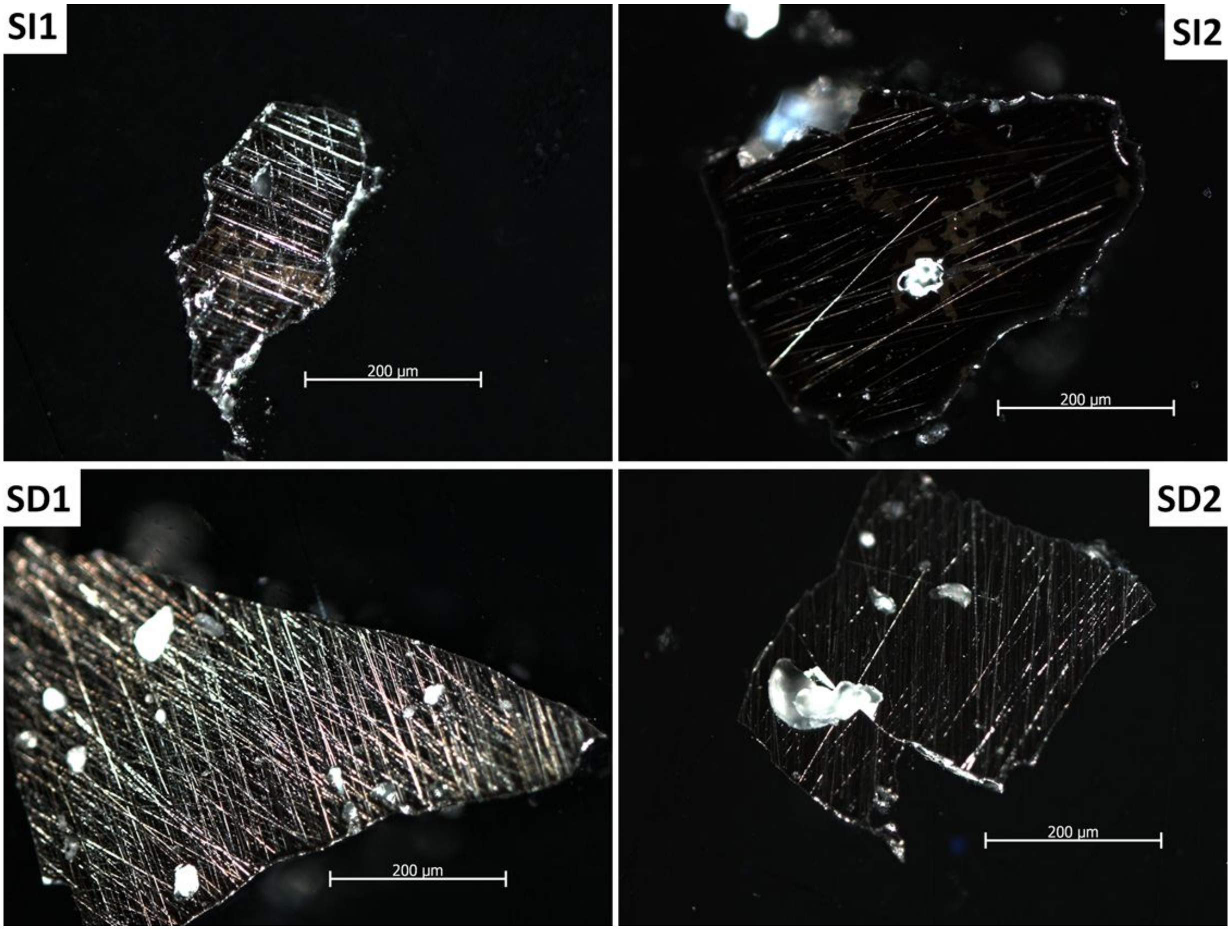

Figure S6 - Reflected light images of the four synthetic quasicrystals (icosahedral phase: SI1 and SI2; decagonal phase: SD1 and SD2) investigated. Scale bar is indicated.

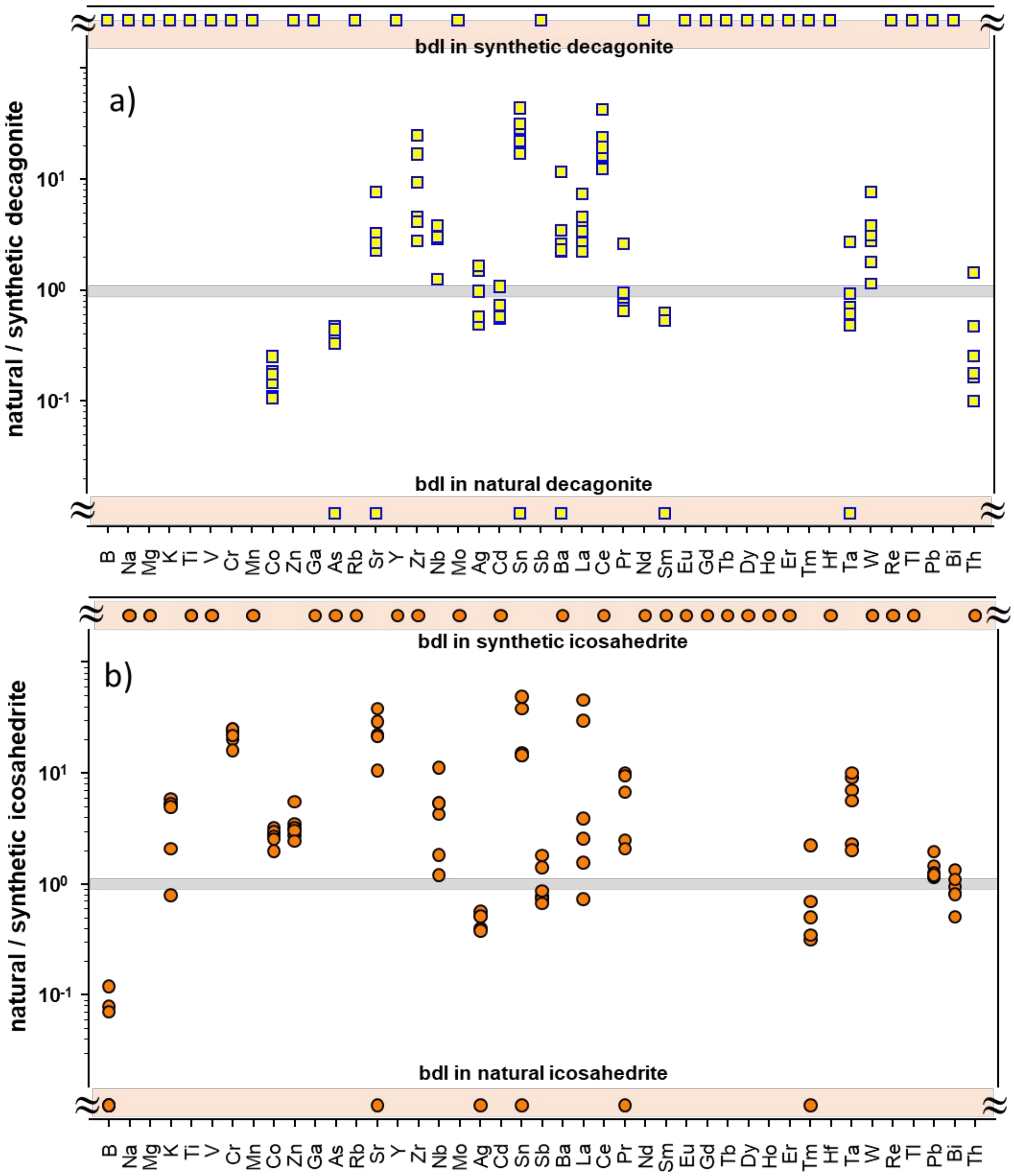

Figure S7 - Elemental content in natural QC ratioed to synthetic QC (decagonite (a), icosahedrite (b)). The elemental content of each data point of the two natural QCs (Table 2) has been divided by the average content of the two synthetic QCs (Table S5). In both panels, those elements below detection limit in synthetic QCs are plotted to the top off-scale light coloured area, whereas those elements below detection limit in natural QCs are plotted to the bottom off-scale light coloured area. Most of the elements occurring in natural QCs are below detection limit in synthetic QCs (see also Table S5). Other elements do not have any correspondence among natural and synthetic QCs as demonstrated by the significant deviation from the thick grey line at 10^0. (i.e., content in natural QC divided by content in synthetic QC equal to unity).

Table S4 – Electron microprobe analyses (elemental wt.% and normalized atomic%) of synthetic icosahedral and decagonal quasicrystals.

	SI1				mean	SI2				mean
	1	2	3	4		1	2	3	4	
	wt.%					wt.%				
Al	42.66	43.56	43.15	43.09	43.12	43.38	42.78	42.99	43.05	43.05
Cu	38.91	38.16	38.55	38.79	38.60	38.24	38.71	39.05	38.41	38.60
Ni	-	-	-	-	-	-	-	-	-	-
Fe	17.99	18.26	17.95	18.19	18.10	18.33	17.79	18.06	18.07	18.06
Total	99.56	99.98	99.65	100.07	99.82	99.95	99.28	100.10	99.53	99.71
	atomic %					atomic %				
Al	62.85	63.51	63.28	63.18	63.21	63.35	63.09	62.95	63.23	63.16
Cu	24.34	23.62	24.00	24.01	23.99	23.71	24.24	24.28	23.95	24.04
Ni	-	-	-	-	-	-	-	-	-	-
Fe	12.81	12.87	12.72	12.81	12.80	12.94	12.67	12.78	12.82	12.80

	SD1				mean	SD2				mean
	1	2	3	4		1	2	3	4	
	wt.%					wt.%				
Al	52.41	51.88	52.34	52.26	52.22	52.09	52.55	52.14	51.80	52.15
Cu	-	-	-	-	-	-	-	-	-	-
Ni	40.15	39.94	39.10	38.92	39.53	39.19	39.55	39.94	39.64	39.58
Fe	7.85	8.08	8.55	8.40	8.22	8.25	7.88	8.45	8.11	8.17
Total	100.41	99.90	99.99	99.58	99.97	99.53	99.98	100.53	99.55	99.90
	atomic %					atomic %				
Al	70.20	69.97	70.31	70.42	70.23	70.31	70.50	69.91	70.06	70.20
Cu	-	-	-	-	-	-	-	-	-	-
Ni	24.72	24.76	24.14	24.11	24.43	24.31	24.39	24.62	24.64	24.49
Fe	5.08	5.27	5.55	5.47	5.34	5.38	5.11	5.47	5.30	5.31

footnote: SI: synthetic icosahedrite, SD: synthetic decagonite;

Table S5 – Trace element analyses (μg/g) of synthetic icosahedrite and decagonite.

		icosahedrite			decagonite			
	LOD	SI1 01	SI2 01	SI2 02	SD1 01	SD1 02	SD2 01	SD2 02
B	(2.7 - 6.2)	54 ± 15	58 ± 10	60 ± 6	-	-	-	-
Na	(14 - 41)	-	-	-	-	-	-	-
Mg	(1.6 - 5.5)	-	-	-	-	-	-	-
K	(4.3 - 5.4)	< 8.9	-	-	-	-	-	-
Ti	(2.6 - 8.6)	-	-	-	-	-	-	-
V	(0.26 - 0.66)	-	-	-	-	-	-	-
Cr	(2.7 - 4.5)	< 5.2	-	-	-	-	-	-
Mn	(3.1 - 6.1)		-	-	-	-	-	-
Co	(0.22 - 0.53)	< 1.7	-	-	15.3 ± 1.1	14.8 ± 0.9	13.1 ± 1.9	14.3 ± 0.7
Zn	(1.1 - 1.8)	35.9 ± 5.4	33.4 ± 3.6	46.7 ± 4.1	-	-	-	-
Ga	(0.24 - 0.33)	-	-	-	-	-	-	-
As	(1.2 - 1.9)	-	-	-	< 3.5	-	-	-
Rb	(0.14 - 0.29)	-	-	-	-	-	-	-
Sr	(0.015 - 0.05)	< 0.036	< 0.058	< 0.026	-	-	< 0.103	< 0.026
Y	(0.05 - 0.09)	-	-	-	-	-	-	-
Zr	(0.05 - 0.08)	-	-	-	0.16 ± 0.10	< 0.085	< 0.13	< 0.063
Nb	(0.02 - 0.08)	-	< 0.045	-	-	-	< 0.18	-
Mo	(0.33 - 0.65)	-	-	-	-	-	-	-
Ag	(0.1 - 0.3)	15.2 ± 3.9	12.8 ± 1.1	15.7 ± 3.1	-	-	-	< 0.14
Cd	(0.5 - 0.8)	-	-	-	< 0.95	-	< 1.9	< 0.62
Sn	(0.2 - 0.3)	1.86 ± 0.72	1.59 ± 0.36	3.07 ± 0.83	< 0.35	-	-	-
Sb	(0.39 - 0.62)	< 1.24	< 0.80	< 0.80	-	-	-	-
Ba	(0.04 - 0.1)	-	-	-	< 0.14	< 0.06	< 0.22	-
La	(0.006 - 0.02)	-	< 0.022	-	0.101 ± 0.064	-	< 0.075	< 0.024
Ce	(0.005 - 0.012)	-	-	-	< 0.03	< 0.024	< 0.032	< 0.018
Pr	(0.009 - 0.031)	< 0.015	-	-	< 0.04	-	< 0.08	-
Nd	(0.26 - 0.52)	-	-	-	-	-	-	-
Sm	(0.03 - 0.18)	-	-	-	-	-	-	0.131 ± 0.088
Eu	(0.01- 0.06)	-	-	-	-	-	-	-
Gd	(0.03 - 0.1)	-	-	-	-	-	-	-
Tb	(0.01 - 0.02)	-	-	-	-	-	-	-
Dy	(0.02 - 0.1)	-	-	-	-	-	-	-
Ho	(0.005 - 0.01)	-	-	-	-	-	-	-
Er	(0.016 - 0.052)	-	-	-	-	-	-	-
Tm	(0.007 - 0.02)	< 0.032	-	-	-	-	-	-
Hf	(0.02 - 0.05)	-	-	-	-	-	-	-
Ta	(0.005 - 0.01)	-	< 0.01	-	< 0.023	-	-	-
W	(0.11 - 0.3)	-	-	-	< 0.28	< 0.35	-	< 0.16
Re	(0.02 - 0.06)	-	-	-	-	-	-	-
Tl	(0.02 - 0.04)	-	-	-	-	-	-	-
Pb	(0.08 - 0.20)	3.3 ± 2.5	3.0 ± 1.1	5.1 ± 2.2	-	-	-	-
Bi	(0.05 - 0.10)	1.00 ± 0.75	1.13 ± 0.38	1.99 ± 0.73	-	-	-	-
Th	(0.008 - 0.025)	-	-	-	0.17 ± 0.12	0.084 ± 0.051	< 0.08	0.033 ± 0.022

footnote: each single spot analysis is given with associated error (1σ). Elemental concentrations reported as *"< value"* are at semi-quantitative level (C^{el} - 1σ < LOD, see results section of text); LOD: range (μg/g) of limit of detection during analytical session; - : below detection limit.